JOURNAL OF CATALYSIS 145, 256–266 (1994)

On the Mechanism of *n*-Butane Oxidation to Maleic Anhydride on VPO Catalysts

I. A Kinetics Study on a VPO Catalyst as Compared to VPO Reference Phases

Y. Zhang-Lin,* M. Forissier,† R. P. Sneeden,* J. C. Védrine,* and J. C. Volta*

*Institut de Recherches sur la Catalyse, CNRS, 2 Avenue A. Einstein, 69626, Villeurbanne, Cédex, France; and †Génie catalytique des Réacteurs de Raffinage, CNRS-ELF, CRES, BP 22, 69360, St. Symphorien d'Ozon, France

Received February 19, 1993; revised June 17, 1993

In order to obtain more information on the mechanism of butane oxidation, the oxidation of *n*-butane, butadiene, furan, and maleic anhydride (MA) is studied on different VPO structures: α_{II}, β, γ, and δ $VOPO_4$, on the one hand, and $(VO)_2P_2O_7$ and the activated VPO catalyst, on the other hand. A general scheme is proposed for the oxidation of butane on these different structures. A direct route to maleic anhydride which implies alkoxide intermediates without desorption in the gas phase of butene, butadiene, and furan is proposed as an alternative to the olefinic route. The activated VPO catalyst is more selective to MA than is $(VO)_2P_2O_7$, while α_{II} $VOPO_4$ dehydrogenates to butadiene. β $VOPO_4$ gives mainly CO_x, while γ and δ $VOPO_4$ are fairly selective to MA.

INTRODUCTION

Most of the maleic anhydride produced worldwide is now obtained by direct catalytic oxidation of butane on the phosphorus vanadium oxide catalyst (VPO). The study of this system has been the subject of extended research, both for industrial reasons, due to the economic importance of maleic anhydride as a chemical intermediate, and for fundamental reasons, as this reaction is very complex, with eight H-abstractions, three O-insertions, and subsequent electron transfers. Three main reviews have been devoted to this catalytic system (1–3). If the physicochemical approach of the VPO system has been extensively developed, as can be seen from the numerous publications in this area in the last 5 years, then few studies have been devoted to the kinetics and the mechanism of this reaction (4–6). In our opinion, the main reason for this is the many possible reaction pathways and the absence of well-identified intermediates in steady-state conditions as compared to the oxidation of 1-butene (2, 6). Though it has been shown that it is not possible to reliably compare the olefin and paraffin kinetic constants on the same VPO surface, it has been suggested that the oxidation of *n*-butane may proceed without intermediate desorption from the active site (7), instead of through a preliminary dehydrogenation step to butenes and subsequent oxidation to maleic anhydride (2). The density of oxidizing sites has been considered as a tool for modifying the selectivity in reactions of mild oxidation (8) and this can be controlled by the catalytic conditions (butane/air ratio, temperature of reaction, contact time). The identification of the effective sites is, however, still under discussion.

There are many discrepancies in the open literature concerning the nature of the active phase. Most of the kinetic studies have been drawn toward the vanadyl pyrophosphate phase, which is considered to be the active phase for butane oxidation to maleic anhydride (4–6). In the former study (4), it was concluded that $(VO)_2P_2O_7$ catalyzes the oxidation of butane to maleic anhydride via redox reaction of its surface layer according to a Mars and Van Krevelen mechanism. V(IV) at the surface of pyrophosphate is proposed to activate molecular oxygen, while the surface layer can be oxidized to a certain extent to V(V), which provides the capacity to oxidize adsorbed hydrocarbons. In the latter study (6), the reactivity of the various oxygen species was examined by thermogravimetric techniques and transient reaction studies. It was shown that intermediates such as butene, butadiene, and furan desorb when the $(VO)_2P_2O_7$ catalyst works in more reducing conditions (high hydrocarbon/O_2 ratio). Furan is readily converted to maleic anhydride on a partially oxidized surface. These results suggest that there are several active oxygen species involved: activated oxygen (O*), which was suggested to be formed by the irreversible dissociative chemisorption of dioxygen via oxidation of V^{4+} to surface V^{5+}, was considered to be responsible for the oxidation of the C–H bonds of butane and furan, while

0021-9517/94 $5.00

a surface lattice oxygen anion should be responsible for allyl oxidation and ring insertion (6).

In a previous publication (9), we showed that catalysts consisting of mixtures of $(VO)_2P_2O_7$ with γ $VOPO_4$ were more efficient for butane oxidation to maleic anhydride than was $(VO)_2P_2O_7$ alone. A study by laser Raman spectroscopy of the activation of the $VOHPO_4 \cdot 0.5H_2O$ precursor showed that α_{II}, γ, and δ $VOPO_4$ structures were generated with $(VO)_2P_2O_7$ while catalytic performances were improving (10). In parallel, δ $VOPO_4$ was observed to transform to α_{II} $VOPO_4$ in the course of the reaction (11). Moreover, butane/air activation of a $(VO)_2P_2O_7$ catalyst prepared in an argon atmosphere showed an improvement of the maleic anhydride yield, while a redistribution of the V^{5+} entities was simultaneously observed on the $(VO)_2P_2O_7$ matrix, as evidenced by ^{31}P MAS–NMR (12). We thus consider that V^{5+} sites organized as $VOPO_4$ phases detectable by XRD or small size $VOPO_4$ structures detectable only by Raman or ^{31}P MAS–NMR should participate on the $(VO)_2P_2O_7$ matrix for the mechanism of butane oxidation to maleic anhydride. Such a hypothesis should be in agreement with the previous studies (6, 8).

In order to bring new information on the reaction scheme and, more precisely, on the respective role of the V^{4+} and V^{5+} species in the different pathways of butane oxidation to maleic anhydride, the present work compares a classical VPO catalyst (V^{4+}-based system) to the pure reference phases $(VO)_2P_2O_7$ (V^{4+} system), α_{II}, β, γ, and δ $VOPO_4$ in the reaction of mild oxidation of butane, butadiene, and furan studied at various temperature and contact times with low substrate partial pressure.

EXPERIMENTAL

Preparation and characterization of the reference phases have been described elsewhere (11). We recall here the main information.

Preparation of Reference Phases

Pure VPO phases were prepared from the three precursors: $VOPO_4 \cdot 2H_2O$, $NH_4(VO_2)_2PO_4$, and $VO(HPO_4) \cdot 0.5\ H_2O$. $(VO)_2P_2O_7$ was obtained by dehydration of $VO(HPO_4) \cdot 0.5H_2O$ under dry nitrogen at 700°C for 6 h (heating rate 75°C $\cdot$ h^{-1}). α_{II} $VOPO_4$ was prepared from $VOPO_4 \cdot 2H_2O$ by dehydration in dry air at 750°C for 17 h (heating rate 240°C $\cdot$ h^{-1}). β $VOPO_4$ was obtained by decomposition of $NH_4(VO_2)_2PO_4$ in dry air at 600°C for 10 h (heating rate 75°C $\cdot$ h^{-1}). γ $VOPO_4$ was prepared by oxydehydration of $VO(HPO_4) \cdot 0.5H_2O$ at 680°C for 4 h under dry oxygen (heating rate 110°C $\cdot$ h^{-1}). δ $VOPO_4$ was obtained from $VO(HPO_4) \cdot 0.5H_2O$ by oxydehydration in dry oxygen at 450°C for 168 h (heating rate 60°C $\cdot$ h^{-1}). These conditions led to crystallized materials. The conditions of preparation from the precursors were mostly in agreement with previous publications (15).

TABLE 1

BET Area of Catalysts (after Preparation)

Catalyst	BET area (m^2/g)
"VPO"	22.5
$(VO)_2P_2O_7$	2.0
α_{II} $VOPO_4$	1.2
β $VOPO_4$	1.8
γ $VOPO_4$	8.7
δ $VOPO_4$	14.0

Preparation of the VPO Catalyst

The VPO catalyst was prepared from $VO(HPO_4) \cdot 0.5H_2O$ as described in Ref. (12). Activation was performed at 440°C under the catalytic atmosphere (1.2% Butane/air) (VSHV = 1200 h^{-1}) with helium as the diluting gas ($C_4H_{10}/O_2/He$ = 1.2/16.4/82.4) for 25 h. The flow rate was 20 cm^3/min. These conditions corresponded to an "equilibrated catalyst" since catalytic results obtained with the previous conditions and physicochemical characteristics as measured by XRD, ^{31}P MAS–NMR, and Raman spectroscopy were unchanged with time of activation after cooling the catalyst to room temperature (12).

After preparation, the VPO catalyst and VPO reference phases were stored under dry argon in order to avoid any rehydration to $VOPO_4 \cdot 2H_2O$, which is observed principally for α_{II}, γ, and δ $VOPO_4$ (18).

Reference Phases and Catalyst Characterization

Prior to the catalytic tests, the samples were characterized by XRD, ^{31}P MAS–NMR as previously described (11), and BET area measurements. BET area of the solids was measured by adsorption of nitrogen at 77.4 K according to the Brunauer–Emmet–Teller method with an automatically controlled apparatus built in our laboratory. No porosity was observed for all materials in the 2–12 nm domain. Table 1 presents the BET surface area of the prepared catalysts. XRD and ^{31}P MAS–NMR spectra are not presented here since they have been published elsewhere (11, 12).

Catalytic Testing

Catalytic test equipment was constructed in order to study the catalytic oxidation at atmospheric pressure of butane, butadiene, furan, and maleic anhydride with the analysis on line of reactants and reaction products. The apparatus was automatically controlled. Sampling valves

were settled in a "hot box" heated at 140°C, while the reactor, the saturator for liquid, and the saturator for solid were set outside and inside the hot box, respectively. We used a classical differential pyrex microreactor (U-tube) with a continuous control of temperature inside the catalytic bed with a thermocouple. Flow rate varied between 20 and 40 $cm^3 \cdot min^{-1}$. The mass of the catalyst used as a powder with a particule diameter lower than 0.5 mm varied from 30 to 600 mg, depending on the catalyst and on the reactant. The reactor was heated by an electrical furnace which was controlled by a temperature programmer. The temperature of the catalytic bed was slowly increased from 100 up to 400–450°C for 40 h. Until 300°C, the temperature was raised by plateaus of 3 h in increments of 50°C and then from 300 up to 450°C in increments of 25°C. From the accuracy of the temperature and the reaction rates, the accuracy for the apparent activation energy determination was estimated to be 5 $kJ \cdot mol^{-1}$. At the end of the catalytic test, the catalyst was cooled at room temperature under the reaction mixture (X/O_2/helium) (X = n-butane, butadiene, furan, and maleic anhydride) prior to physicochemical analyses. This aspect will be presented in a forthcoming publication (19). For gases (butane, butadiene), the composition was controlled with flow meters, while for the liquid (furan) or solid (maleic anhydride), it was done with saturators outside or inside the "hot box," respectively.

Analysis of reactants and products of reaction was performed by on-line gas chromatography. Hydrocarbons were separated on a 4 m × 1/8" (80–100 mesh) Durapak column working at 60°C with an FID detector. Oxygenates were separated on a 2 m = 1/8" (80–100 mesh) 10% AT 1200 column impregnated with 1% H_3PO_4 on Chromosorb WAW working at 90°C with an FID detector. Finally, CO, CO_2, H_2O, O_2, and He (diluting gas) were separated on a 4 m × 1/8" (80–100 mesh) Carbosieve B column working at 100°C with a TCD detector.

For a more detailed analysis, liquid and solid products were trapped in water or acetone cooled at 25 or 0°C, depending on conditions. Condensed products were then analyzed separately by GC–SM coupling. It appeared that, in some cases, the empty reactor was slightly reactive after some catalytic runs. As a consequence, it was decided to systematically wash it with an HCl–HNO_3 solution (aqua regia), then with ammonia, and finally to rinse it with distilled water. Prior to each new run, the reactor was tested alone to be sure that it was inactive. Some runs were performed with a low catalytic mass (<100 mg) in the case of highly reactive molecules. In the latter case, we used a pyrex U-tube which was changed for each run.

For all hydrocarbon feeds, the stability of the reactional activity was verified for all "VPO" and reference phases by replicating the reference measurement.

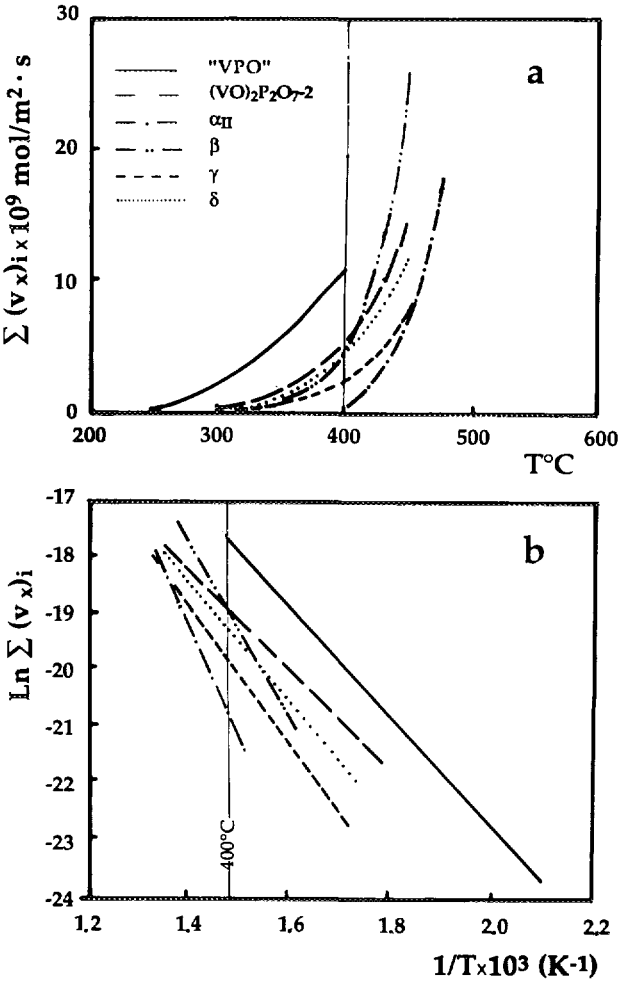

FIG. 1. Intrinsic rates for butane conversion.

RESULTS

Butane Oxidation

Figure 1 presents the results obtained, as function of temperature, for the intrinsic rates $\Sigma(v)_i$ of butane conversion (Fig. 1a) and the corresponding Ln $\Sigma(v)_i$ transformed from which apparent activation energies were calculated in the field of conversion 0–30% (Table 2). Different values suggest that slow steps involved are different depending on the catalysts. The lowest activation energies are observed for "VPO" and $(VO)_2P_2O_7$, while they are higher for the $VOPO_4$ phases according to the order $\alpha_{II} > \beta > \gamma > \delta$. We can conclude that butane activation is easier in the first two catalysts.

Note that the low value observed for δ $VOPO_4$ (87 $kJ \cdot mol^{-1}$), which has been observed to partially transform into α_{II} $VOPO_4$ in these catalytic conditions (11), is nearer the value observed for "VPO" (79 $kJ \cdot mol^{-1}$) than the value observed for α_{II} $VOPO_4$ (167 $kJ \cdot mol^{-1}$), which

TABLE 2

Apparent Activation Energy Values of for *n*-Butane Oxidation for Different Catalysts

Catalyst	Activation energy (kJ · mol^{-1})
"VPO"	79
$(VO)_2P_2O_7$	71
α_{II} $VOPO_4$	167
β $VOPO_4$	125
γ $VOPO_4$	100
δ $VOPO_4$	87

TABLE 3

Activation Energy of the Catalysts for MA Formation from Butane Oxidation

Catalyst	Activation energy (kJ · mol^{-1})
"VPO"	67
$(VO)_2P_2O_7$	67
α_{II} $VOPO_4$	109
β $VOPO_4$	75
γ $VOPO_4$	71
δ $VOPO_4$	67

should suggest a peculiar structure for α_{II} coming from the transformation of δ $VOPO_4$ as compared to classical α_{II} as previously described.

Figure 2 gives the results obtained for the intrinsic rates of maleic anhydride $v(_{MA})_i$ formation (Fig. 2a) and the corresponding Ln $v(_{MA})_i$ (Fig. 2b) as a function of temperature.

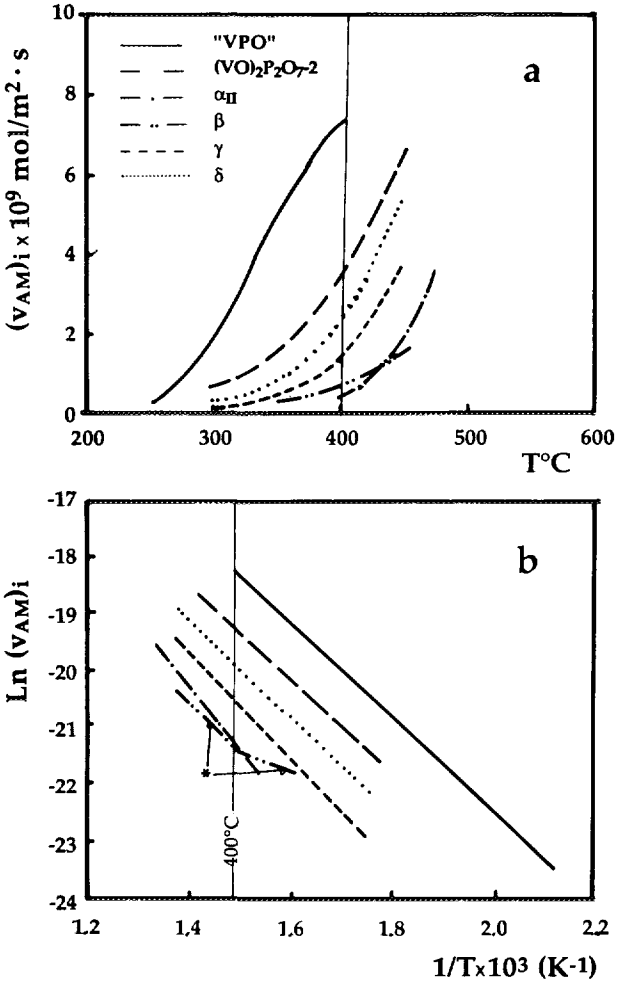

FIG. 2. Intrinsic rates for MA formation during butane oxidation.

"VPO" catalyst presents the highest rate as compared to $(VO)_2P_2O_7$ and the $VOPO_4$ phases. The apparent activation energies for MA formation (Table 3) are systematically lower than the corresponding values for butane oxidation (Table 2), which probably means that the true activation energy for MA formation from butane is lower than that of the other products and CO and CO_2 from MA. This observation is not incompatible with a direct route from butane to MA. The apparent activation energies (Table 3) are quite similar for "VPO," $(VO)_2P_2O_7$, γ, and δ $VOPO_4$. This is particularly noteworthy for the two last structures, which appear favorable for MA formation. The highest value observed for α_{II} $VOPO_4$ (109 kJ · mol^{-1}) has to be related to the highest value observed for butane conversion on this catalyst (Table 2). This result should be in favor of a different way of formation of MA on this structure as compared to the other catalysts. A different behavior is observed for β $VOPO_4$, below and above 400°C, and should correspond to a superficial evolution of this catalyst at high temperature, as evidenced from the physicochemical study before and after the catalytic run (19).

To summarize, at 400°C and at a given temperature, "VPO" and $(VO)_2P_2O_7$ are the best catalysts for *n*-butane oxidation to maleic anhydride (MA). γ and δ $VOPO_4$ catalysts have similar catalytic behaviors: surprisingly, they are quite selective for MA formation and give few butenes and butadiene (C_4). In contrast, α_{II} and β $VOPO_4$ catalysts present a lowest MA selectivity and give mainly C_4 for α_{II}, and CO and CO_2 for β $VOPO_4$.

Butadiene Oxidation

It is known that butadiene oxidation can be responsible to some catalyst deactivation (2). We verified that under our experimental conditions the deactivation was lower than 20% after 30 h of time on stream and thus can be disregarded.

At the temperature of butane oxidation (400–430°C) and under the same reaction conditions, conversion of butadiene on "VPO," γ, and δ $VOPO_4$ is nearly total,

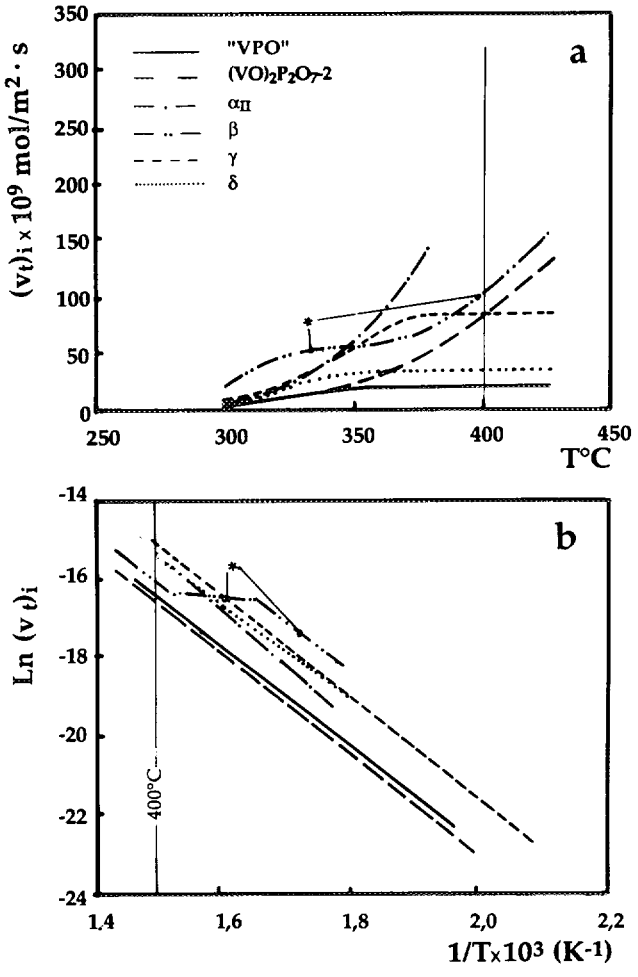

FIG. 3. Intrinsic rates for butadiene conversion.

showing that butadiene reacts with a much higher rate than butane. However, a comparison between the different samples can be done from the curves $\mathrm{Ln}(v_t)_i = f(1/T)$ (Fig. 3b) drawn from measurements realized at low temperature and extrapolated at higher temperatures. With the exception of β $VOPO_4$, which gives a nonlinear curve due to a structural modification of the catalyst during reaction (19), comparison of the intrinsic rates for butadiene conversion at 400°C gives the following order:

$$\gamma\ VOPO_4 > \delta\ VOPO_4 = \alpha_{II}\ VOPO_4 > \text{"VPO"} > (VO)_2P_2O_7.$$

Note, in this case, a classification reversed as compared to butane oxidation. Table 4 shows that activation energies measured in a conversion field 0–30% for butadiene conversion are mainly similar. They are larger than the apparent activation energies measured for butane oxidation except for α_{II} $VOPO_4$. This fact can be interpreted by the possibility of a mechanism which implies a butadiene intermediate. The first step butane–butadiene is rate limiting and particularly sensitive to oxide structure, but it does not permit one to refute a direct butane–MA mechanism.

A comparison to butane oxidation shows that with the

TABLE 4

Activation Energy of the Catalysts for Butadiene Conversion

Catalyst	Activation energy (kJ · mol^{-1})
"VPO"	105
$(VO)_2P_2O_7$	105
α_{II} $VOPO_4$	113
β $VOPO_4$	105
γ $VOPO_4$	109
δ $VOPO_4$	100

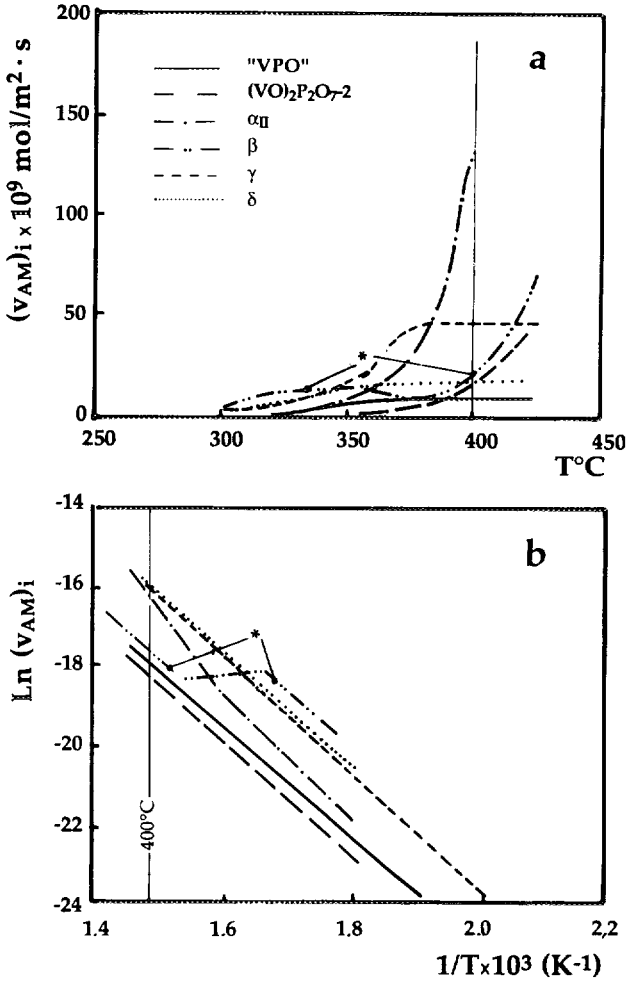

FIG. 4. Intrinsic rates for MA formation during butadiene oxidation.

TABLE 5

Apparent Activation Energy Values for MA Formation from Butadiene Oxidation for Different Samples

Catalyst	Activation energy (kJ · mol^{-1})
"VPO"	125
$(VO)_2P_2O_7$	127
α_{II} $VOPO_4$	130 (<350°C)
	159 (>350°C)
β $VOPO_4$	125 (<325°C)
γ $VOPO_4$	121
δ $VOPO_4$	119

exception of α_{II} $VOPO_4$ all catalysts show a higher activation energy, suggesting a more difficult reaction pathway in the case of butadiene oxidation. A comparison of the intrinsic rates for MA formation can be done from the curves $\text{Ln}(v_{AM})_i = f(1/T)$ (Fig. 4b).

At 400°C, the corresponding order is observed:

$$\delta\ VOPO_4 = \gamma\ VOPO_4 > \alpha_{II}\ VOPO_4 > \beta\ VOPO_4 > \text{"VPO"} > (VO)_2P_2O_7.$$

Note that as for butane oxidation, the straight line for β $VOPO_4$ changes with temperature. A break is observed for the line characteristic of α_{II} $VOPO_4$ at 350°C, with an increase of the slope beyond this temperature. This phenomenon has to be related with an α_{II} $VOPO_4$–γ $VOPO_4$ structural evolution (19) which favors MA formation. Apparent activation energies for MA formation are given in Table 5 (conversion lower than 30%). The values are similar for all catalysts (119–130 kJ · mol^{-1}), which suggests that the slow step and the structure of the active sites are comparable. In this case, the activation energies for MA formation are higher than those for the overall reaction. MA selectivity may increase with temperature.

The comparison (Fig. 5b) for the furan formation variations of the $\text{Ln}(v_F)_i$ versus $(1/T)$ shows that at low temperatures (300–325°C), β $VOPO_4$ presents the higher rate, while at 400°C the corresponding order is observed:

$$\alpha_{II}\ VOPO_4 > \gamma\ VOPO_4 = \delta\ VOPO_4 > (VO)_2P_2O_7 > \text{"VPO."}$$

The $VOPO_4$ catalysts present higher rates for furane formation as compared to the vanadyl pyrophosphate based catalysts $(VO)_2P_2O_7$ and "VPO." Moreover, it appears that the δ $VOPO_4$ catalyst, which presents the higher rate for MA formation as compared to the α_{II} and γ $VOPO_4$ catalysts, less efficiently transforms furan.

To summarize, it appears that the catalytic behavior of the different catalysts strongly depends on the temperature considered. With the exception of β $VOPO_4$, the $VOPO_4$ catalysts show, for butadiene oxidation, and in the common 400–430°C range of butane oxidation, a selectivity for MA comparable to the vanadyl pyrophosphate based catalysts and a higher yield. The two γ and δ $VOPO_4$ catalysts show a similar behavior. They show higher activity and selectivity to MA as compared to α_{II} $VOPO_4$. These catalysts appear to be transformed in catalytic conditions (19). For the vanadyl pyrophosphate-based catalysts $(VO)_2P_2O_7$ and "VPO," butadiene oxidation to MA is much less selective than butane oxidation, which suggests that the oxidation of butane to MA should occur according a route different from that of the oxidation of butadiene. For all catalysts, furan appears to be an intermediate for the oxidation of butadiene to MA.

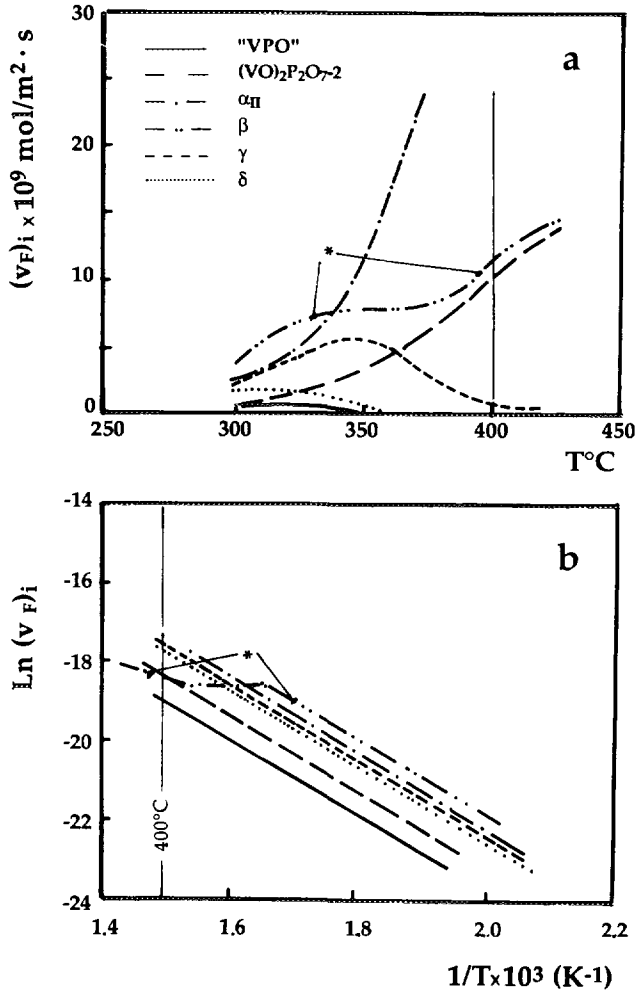

FIG. 5. Intrinsic rates for furan formation from butadiene oxidation.

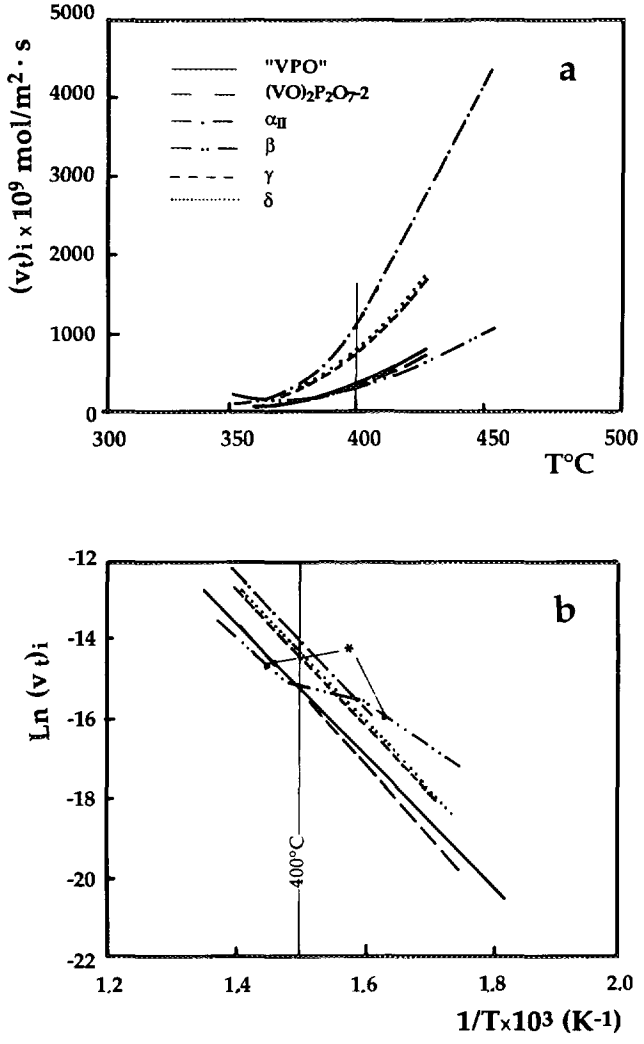

FIG. 6. Intrinsic rates for furan conversion.

Furan Oxidation

The evolution of the intrinsic rates $(v_t)_i$ for furan transformation in the 400–430°C temperature range of butane oxidation shows the corresponding order (Fig. 6a):

$$\alpha_{II}\ VOPO_4 > \delta\ VOPO_4 = \gamma\ VOPO_4 > \text{"VPO"} = (VO)_2P_2O_7 = \beta\ VOPO_4.$$

The variation Ln $(v_t)_i$ versus (1/T) (Fig. 6b) show similar slopes with the exception of β $VOPO_4$ for which a transformation of the solid was observed as for butane and butadiene oxidation. Corresponding calculated activation energies are given in Table 6 (conversion lower than 30%).

The order of the intrinsic rates for MA formation is the same as that observed for furan conversion (Fig. 7):

TABLE 6

Apparent Activation Energy Values for Furan Conversion for Different Samples

Catalyst	Activation energy (kJ · mol^{-1})
"VPO"	132
$(VO)_2P_2O_7$	138
α_{II} $VOPO_4$	134
β $VOPO_4$	105 (300°C < T < 350°C) 128 (T > 350°C)
γ $VOPO_4$	134
δ $VOPO_4$	130

$$\alpha_{II}\ VOPO_4 > \delta\ VOPO_4 = \gamma\ VOPO_4 > \text{"VPO"} = (VO)_2P_2O_7 = \beta\ VOPO_4.$$

The variation Ln $(v_t)_i$ versus $(1/T)$ (Fig. 7b) shows, in this case, different activation energies as it is shown in Table 7.

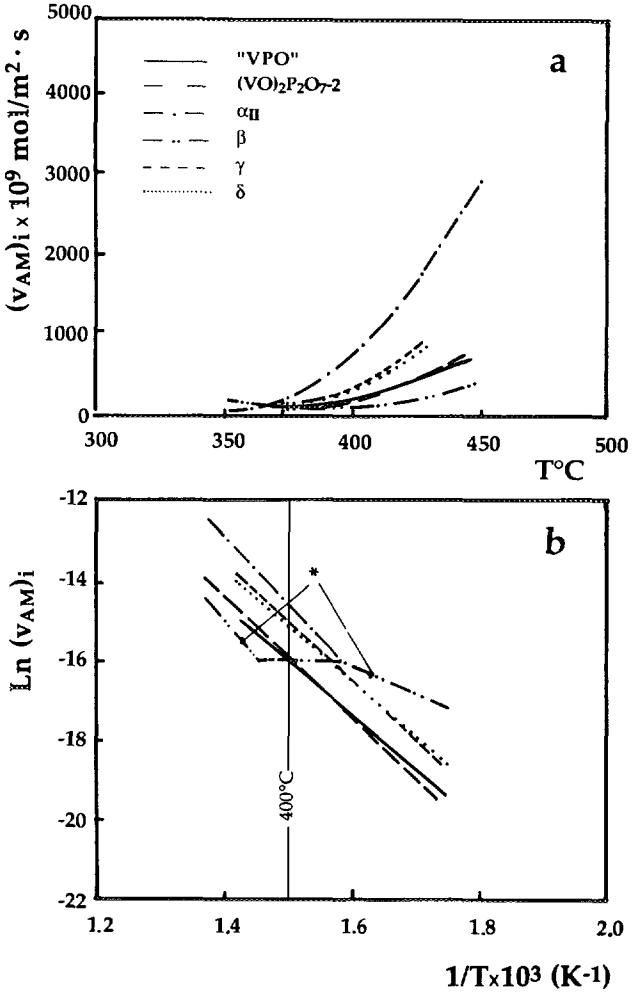

FIG. 7. Intrinsic rates for MA formation during furan oxidation.

TABLE 7

Apparent Activation Energy Values of the Catalysts for MA Formation from Furan Conversion

Catalyst	Activation energy (kJ · mol^{-1})
"VPO"	109
$(VO)_2P_2O_7$	125
α_{II} $VOPO_4$	148
β $VOPO_4$	100 (300°C < T < 350°C)
	146 (T > 350°C)
γ $VOPO_4$	128
δ $VOPO_4$	113

To summarize, in the range of butane oxidation (400–430°C), it appears that, for furan oxidation, the α_{II}, γ, and δ $VOPO_4$ catalysts show a higher activity and a higher selectivity for MA formation as compared to the "VPO" and $(VO)_2P_2O_7$ catalysts. On the contrary, β $VOPO_4$ favors total oxidation. As a consequence, if furan is an intermediate in butane oxidation to maleic anhydride at 400°C, the presence of the α_{II}, γ, and δ $VOPO_4$ phases simultaneously with the $(VO)_2P_2O_7$ structures should be favorable for MA formation.

Maleic Anhydride Oxidation

In order to evaluate the behavior of the different VPO samples for the degradation of maleic anhydride, the different catalysts have been compared in conditions similar to that of butane oxidation, that is, with comparable partial pressures of maleic anhydride formed. Partial pressures of MA have been controlled from the temperature of a saturator set in the "hot box" of the catalytic test equipment. The composition was $MA/O_2/He$ = 0.9/13.1/86.0. CO and CO_2 were the only detected products with a good carbon balance (97%). Measurements were performed at 350 and 400°C with conversion ranging from 2 up to 22%, depending on the catalysts. Results are given in Table 8.

With the exception of δ $VOPO_4$, the rate for the oxidation of MA is the lowest for VPO. Note that it is slightly higher for $(VO)_2P_2O_7$ than for VPO and the highest for β $VOPO_4$ in the case of the $VOPO_4$ structures. These results are in agreement with those observed in the case of butane oxidation, for which β $VOPO_4$ was shown to favor total oxidation.

DISCUSSION

This study gives interesting information on the mechanism of butane oxidation and about the structures which are important at the different intermediate steps going from butane to maleic anhydride. It has been proposed previously that the reaction proceeds through the formation of butene, butadiene, and furan according to an olefinic route (1, 2). However, these intermediates are never detected at low butane/oxygen ratios, which are conditions currently used in industry for maleic anhydride synthesis. Thus, the desorption of the olefinic intermediates is questionable, and we can imagine another route which may imply more attached intermediates so that the whole scheme of oxidation of the butane molecule may occur at the surface of the catalysts grains without desorption (7). From the results obtained with the conversion of each reactant versus the different possible oxidation products, it is possible to estimate a direct possible pathway on each structure. For this calculation, the following hypotheses have been considered:

—Each molecule detectable in the gaseous phase can be a reaction intermediate or a final product.

—The reaction intermediates are thought to be in equilibrium in the gaseous phase.

—All reactions are supposed to be hydrocarbon first order. This hypothesis is justified due to the fact that partial pressures of reactants are always low ($<0.016 \times 10^5$ Pa) as compared to oxygen ($>0.16 \times 10^5$ Pa). Moreover, no reduction of the catalyst was observed after reaction (19).

—The rate constants are not modified by the presence

TABLE 8

Catalytic Results for MA Oxidation Measured at 350 and 400°C

	Conversion (%)		$\sigma(v_{MA})_i \times 10^9$ (mol/m^2 · s)		$(v_{CO})_i \times 10^9$ (mol/m^2 · s)		$(v_{CO_2})_i \times 10^9$ (mol/m^2 · s)	
Catalyst	350°C	400°C	350°C	400°C	350°C	400°C	350°C	400°C
"VPO"	10.0	22.5	0.4	1.7	0.3	0.9	0.1	0.8
$(VO)_2P_2O_7$	2.0	5.0	0.9	2.2	0.5	1.2	0.4	1.0
α_{II} $VOPO_4$	2.5	6.3	1.7	5.7	0.8	2.8	0.9	3.0
β $VOPO_4$	8.0	18.0	7.8	16.4	3.2	5.1	4.6	11.3
γ $VOPO_4$	2.5	6.2	1.0	2.3	0.3	0.6	0.4	1.0
δ $VOPO_4$	6.8	11.0	0.5	1.1	0.3	0.6	0.2	0.5

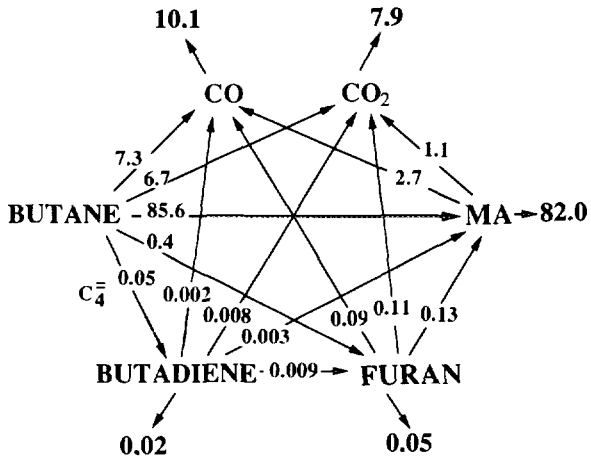

FIG. 8. Reaction scheme for butane oxidation on VPO catalyst at 350°C.

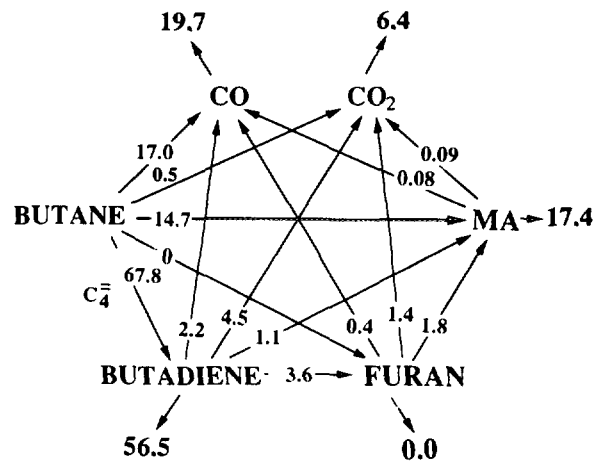

FIG. 10. Reaction scheme for butane oxidation on α_{II} $VOPO_4$ at 350°C.

of another reactant. This implies that there is no effect of fouling by surface polymers or reducing of the catalysts, which should modify the catalytic surface when changing the reactants.

No solid reduction is observed for $(VO)_2P_2O_7$, α_{II}, and γ $VOPO_4$ structures, but β $VOPO_4$ has been observed to be partially reduced into $(VO)_2P_2O_7$ (17) while δ $VOPO_4$ is partially transformed into α_{II} $VOPO_4$ under butane oxidation (9). Nevertheless, as it was impossible to have a quantitative evaluation of these transformations, such a hypothesis was followed.

—The rate of CO oxidation into CO_2 has been supposed low as compared to its rate of formation.

Figures 8–13 give the reaction schemes obtained for the different samples calculated from experimental data given above and measured at 350°C. Numbers associated

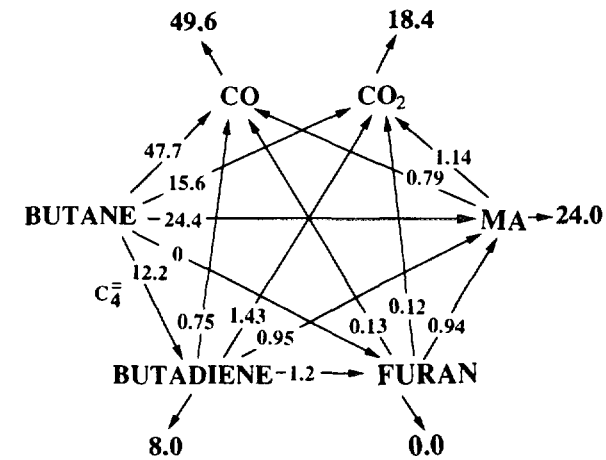

FIG. 11. Reaction scheme for butane oxidation on β $VOPO_4$ at 350°C.

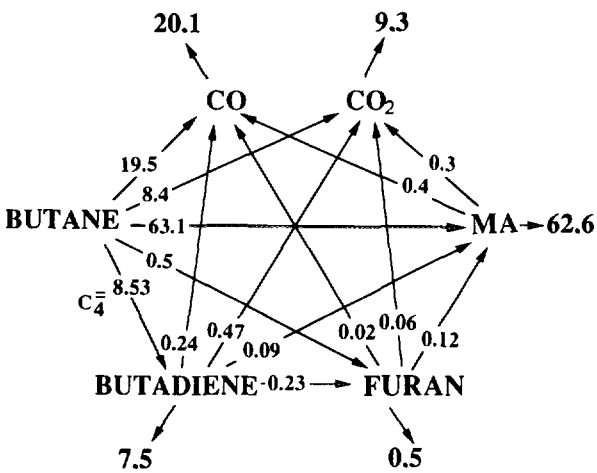

FIG. 9. Reaction scheme for butane oxidation on $(VO)_2P_2O_7$ at 350°C.

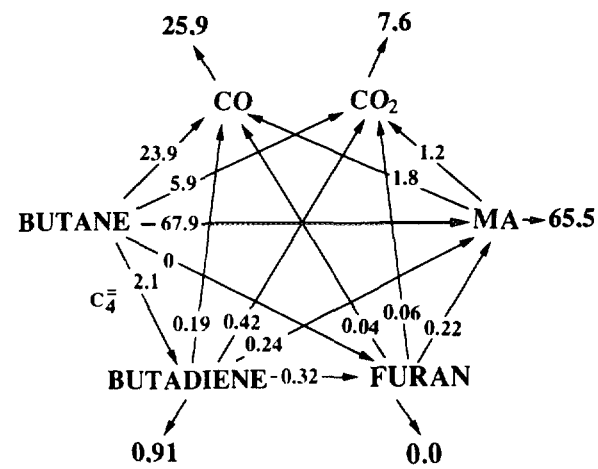

FIG. 12. Reaction scheme for butane oxidation on γ $VOPO_4$ at 350°C.

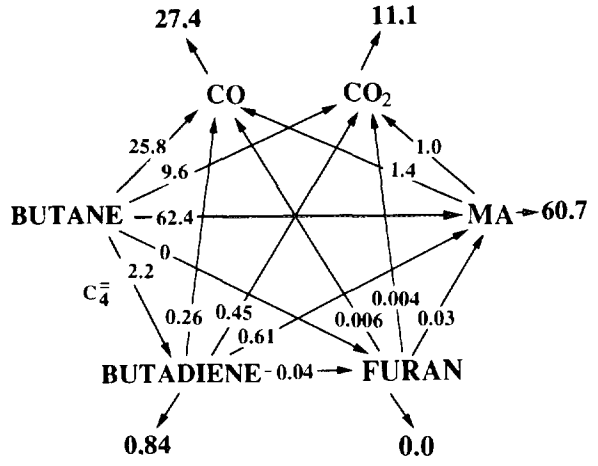

FIG. 13. Reaction scheme for butane oxidation on δ $VOPO_4$ at 350°C.

with arrows directed outside from each reaction product correspond to selectivities measured for each product. Numbers associated with arrows inside the scheme were obtained from calculation, taking into account results obtained for the transformation of each reactant to the intermediates and the further transformation of these ones. As an example, if we consider Fig. 8 for the VPO catalyst, starting from 100 molecules of butane, 7.3 are oxidized into CO, 6.7 into CO_2, 85.6 into MA, 0.4 into furan, and 0.05 into butadiene. The 82.0 mol of MA, which finally are evolved from the reactor and correspond to the measured selectivity for this product, come from the direct oxidation of butane (85.6 mol), from the intermediate oxidation of butadiene (0.003 mol), from the intermediate oxidation of furan (0.13 mol), and from the degradation by oxidation into CO (2.7 mol) and CO_2 (1.1 mol). The same balance can be done for butadiene, furan, CO, and CO_2, which gives the final scheme of Fig. 8.

From the schemes of butane oxidation on the different structures (Figs. 8–13), it can be concluded that:

1. There is a direct route which is the main one from butane to maleic anhydride, which appears from a comparison between the observed selectivity and the calculated one on the butane–MA central arrow.
2. The route which goes through the molecular intermediates butadiene and furan is secondary.
3. The route between butane and furan is negligible, which shows that furan is probably not an intermediate for butane oxidation. However, it appears to be an intermediate for the oxidation of butadiene to MA.
4. The $VOPO_4$ phases give higher concentrations of CO_x, butadiene, and furan than do VPO and $(VO)_2P_2O_7$.
5. The α_{II} $VOPO_4$ structure is highly dehydrogenating into butadiene and poorly selective to MA. β $VOPO_4$ gives mainly CO_x, a result which is well known.
6. The γ and δ $VOPO_4$ structures are surprisingly as selective into MA as $(VO)_2P_2O_7$.
7. The VPO catalyst is observed to be more selective into MA as compared to $(VO)_2P_2O_7$, which is indicative of a different physicochemistry. This aspect will be discussed in a forthcoming publication (19).

The probable direct way from butane to maleic anhydride is compatible with a mechanism implying alkoxide intermediates as previously proposed (7). These alkoxide should maintain a σ-bond between the substrate and the catalyst surface, which could explain that no equilibrium is observed between these intermediates and the gas phase. On the contrary, from butene, π-allyl intermedi-

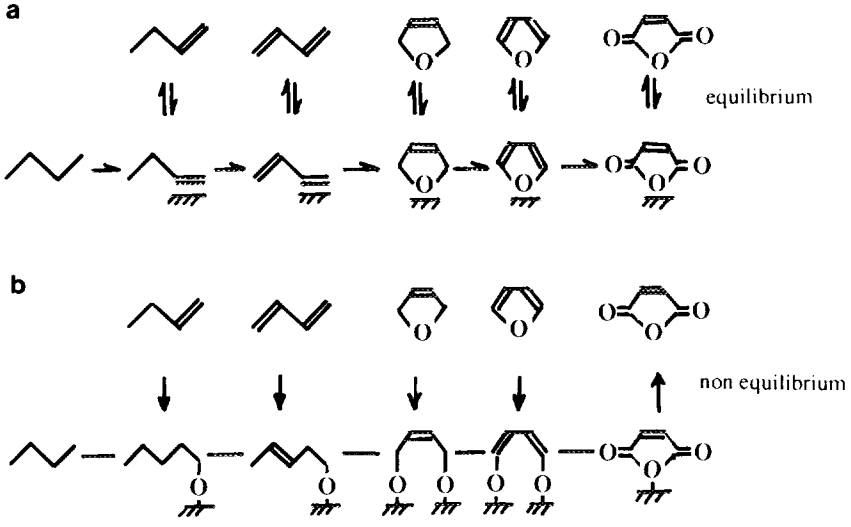

FIG. 14. The two routes for butane oxidation: (a) olefinic and (b) alkoxide.

ates are probably more weakly bonded to the catalyst surface and are thus in equilibrium with the gaseous phase (see Fig. 14). The alkoxide mechanism should be favored by a peculiar local structure of the surface in order to accommodate the specific steric hindrance of the third and fourth steps for furan- and tetrahydrofuran-bonded intermediates (20). The distribution of the oxygen groups and the oxidation state of vanadium at the surface of the catalysts grains should be very important in regulating this mechanism and may change during the activation of the catalyst depending on temperature, O_2/butane ratio, flow rate, and water content in the gas atmosphere. This explains the great differences observed between the different VPO structures. For the olefinic route, the nature of the active phase appears to be less important, since the intermediates may jump from one site to another at each reaction step. These differences will be discussed in a forecoming paper (19).

REFERENCES

1. Hodnett, B. K., *Catal. Rev.-Sci. Eng.* **27,** 373 (1985).
2. Centi, G., Trifiro, F., Ebner, J. R., and Franchetti, V. M., *Chem. Rev.* **88,** 55 (1988).
3. Centi, G. (Ed.), "Vanadyl Pyrophosphate Catalysts," Catalysis Today, Vol. 16. Elsevier, Amsterdam, 1993.
4. Centi, G., Manenti, I., Riva, A., and Trifiro, F., *Appl. Catal.* **9,** 177 (1984).
5. Callahan, J. L., and Grasselli, R. K., *AIChE J.* **9,** 755 (1963).
6. Pepera, M. A., Callahan, J. L., Desmond, M. J., Millberger, E. C., Blum, P. R., and Bremer, N. J., *J. Am. Chem. Soc.* **107,** 4883 (1985).
7. Aguero, A., Sneeden, R. P. A., and Volta, J. C., *in* "Heterogeneous Catalysis and Fine Chemicals" (M. Guisnet, Ed.), Studies in Surface Science and Catalysis, Vol. 41, p. 353. Elsevier, Amsterdam, 1988.
8. Ebner, J. R., and Gleaves, J. T., *in* "Oxygen Complexes and Oxygen Activation by Transition Metals" (A. E. Martell and D. T. Sawyer, Eds.), p. 273. Plenum, New York, 1988.
9. Harrouch Batis, N., Batis, H., Ghorbel, A., Védrine, J. C., and Volta, J. C., *J. Catal.* **128,** 248 (1991).
10. Volta, J. C., Bere, K., Zhang-Lin, Y. J., and Olier, R., *in* "Symposium on Selective Oxidation, ACS Meeting, Washington, DC, 23/8/1992" (S. T. Oyama and J. W. Hightower, Eds.), ACS Symposium Series, Vol. 523, p. 216. ACS, Washington, DC, 1993.
11. Ben Abdelouahab, Olier, R., Guilhaume, N., Lefebvre, F., and Volta, J. C., *J. Catal.* **134,** 151 (1992).
12. Zhang-Lin, Y. J., Sneeden, R. P. A., and Volta, J. C., *in* "Vanadyl Pyrophosphate Catalyst" (G. Centi, Ed.), Catalysis Today, Vol. 16, p. 31. Elsevier, Amsterdam, 1993.
13. Ladwig, G., *Z. Anorg. Chem.* **338,** 266 (1965).
14. Bordes, E., Courtine, P., and Pannetier, G., *Ann. Chim.* **8,** 105 (1973).
15. Bordes, E., and Courtine, P., *J. Catal.* **57,** 236 (1979).
16. Souchay, P., and Dubois, S., *Ann. Chim.* **3,** 88 (1948).
17. Johnson, J. W., Johnston, D. C., Jacobson, A. J., and Brody, J. F., *J. Am. Chem. Soc.* **106,** 8123 (1984).
18. Ben Abdelouahab, F., Olier, R., and Volta, J. C., submitted for publication.
19. Zhang-Lin, Y., Forissier, M., Védrine, J. C., and Volta, J. C., *J. Catal.* **145,** 267 (1994).
20. Ziolkowski, J., Bordes, E., and Courtine, P., *J. Catal.* **122,** 126 (1990).